

Friction-wear behaviors of cathodic arc ion plating AlTiN coatings at high temperatures



Kong Dejun^{a,b,*}, Guo Haoyuan^a

^a College of Mechanical Engineering, Changzhou University, Changzhou 213164, PR China

^b Jiangsu Key Laboratory of Materials Surface Science and Technology, Changzhou University, Changzhou 213164, PR China

ARTICLE INFO

Article history:

Received 25 January 2015

Received in revised form

3 March 2015

Accepted 4 March 2015

Available online 14 March 2015

Keywords:

AlTiN coating

High temperature friction and wear

COF

Wear mechanism

ABSTRACT

An cathodic arc ion plating AlTiN coating was prepared on a YT14 hard alloy. The surface-interface morphologies, the compositions of chemical elements and the phases were analyzed with using SEM (scanning electron microscopy), EDS (energy dispersive spectrometry) and XRD (X-ray diffraction), respectively. Additionally, the surface roughness and grain diameter were observed using AFM (atomic force microscopy). The COFs (coefficients of friction) and wear behaviors of the AlTiN coating were investigated using a high temperature tribological machine at high temperatures (700–900 °C), which were measured with a XM808P type PID temperature control instrument. The results show that the N content of the coating is fully released at high temperatures, and the mixed oxides of Al₂O₃ and TiO₂ are formed, improving the wear resistance and lubricating effect of the AlTiN coating. The average COF of the AlTiN coating at 700 °C, 800 °C and 900 °C is 0.77, 0.65 and 0.57, respectively, showing good tribological properties, the wear mechanisms are primarily composed of oxidation wear and abrasive wear, accompanied with fatigue and adhesive wear.

© 2015 Elsevier Ltd. All rights reserved.

1. Introduction

As the first generation of coating, TiN coatings display many advantages (such as low COF, good friction resistance, and high toughness and hardness [1]). TiN coatings are widely used on cutting tools, molds and the surface modification of mechanical parts. However, the working temperature for the TiN coating oxidation resistance is only 550 °C, which fails to satisfy the requirements of high temperature processing [2–4]. Because of the FCC (face-centered cubic) structure of TiN, the selected Ti atoms are replaced by Al atoms at the TiN lattice, forming AlTiN. This AlTiN maintains the FCC structure, improving the mechanical properties, wear resistance and machinability of TiN. Notably, the anti-oxidation temperature can exceed 800 °C [5–8]. In addition, the dense mixed oxide films of Al₂O₃ and TiO₂ form on the AlTiN coating surface at high temperatures, hindering the diffusion of O atoms into the interior coating and improving the oxidation resistance of the AlTiN coating [9–11]. Multiple studies have been performed on AlTiN coating applications, the friction and wear mechanism of the AlTiN coating has been investigated [12], but the plane scans and contours of worn traces at high temperatures has not been reported. In this study, an AlTiN coating was prepared by CAIP (cathodic arc ion plating), and the COFs

of AlTiN coatings were investigated using a high temperature tribological test. Additionally, the surface morphologies, plane scans and phases of the traces were analyzed with SEM (scanning electron microscopy), EDS (energy dispersive spectroscopy) and XRD (X-ray diffraction), respectively. The results of this study provide an experimental basis for investigating the wear behaviors of the AlTiN coating at high temperatures.

2. Experimental

The substrate material was YT14 hard alloy with a chemical composition as follows (mass, %): WC 78, TiC 14, Co 8. The samples were sequentially polished using 80#, 120#, 200#, 600# and 800# sandpapers and metallographic sandpaper. Before being put into the vacuum chamber, the samples were cleaned with pure acetone using ultrasonic oscillation for 10 min and were dried for the deposition in the PVT coating system. To deposit AlTiN coatings, industrial high purity H₂ and N₂ were used as the working gas, and each alloy target of Al and Ti was adopted with an atom ratio of 50%. The technological parameters of CAIP were as follows: a bias power of –100 V, target electric current of 70 A, duty cycle of 30%, gas pressure of 1.2 Pa, working temperature of 500 °C and deposition time of 60 min. After completion, the surface roughness and grain size were analyzed with a CSPM5500 type AFM (atomic force microscope). The friction and wear tests of the AlTiN coatings were

* Corresponding author at: College of Mechanical Engineering, Changzhou University, Changzhou 213164, PR China. Tel.: +86 15961203760; fax: +86 51981169812.

E-mail address: kong-dejun@163.com (K. Dejun).

conducted on a HT-1000 type high temperature tribological machine (friction mode: sliding; friction pair: $\Phi 6$ ceramic (Si_3N_4) ball; load: 5 N; rotation speed: 500 rpm; radius of gyration: 5 mm; temperature: 700 °C, 800 °C and 900 °C). The worn contours of the AlTiN coating were measured on a CFT-I type reciprocation friction testing machine. The morphologies, plane scans and phases of worn traces were analyzed with a JSM-6360LA type SEM, configured EDS and D/max2500PC type XRD, respectively.

3. Analysis and discussion of results

3.1. Surface morphologies and EDS analysis

Fig. 1(a) shows that the AlTiN coating was a unique blue-gray color with a continuous and uniform structure. Additionally, no shedding phenomenon was displayed, but several white particles of different sizes were noted. Fig. 1(b) shows that the thickness of the AlTiN coating was approximately 1.75 μm . A light and dark interface was noted between the coating and substrate, at which the coating and substrate was closely integrated with no cracking. The EDS analysis result for the AlTiN coating is shown in Fig. 1(c). The mass fractions of three chemical elements (Al, Ti and N) are as follows: Al 41.09, Ti 48.06, N 10.84. Additionally, the atom fractions are as follows: Al 46.12, Ti 30.34, N 23.54. The content of Al atoms was higher than that of Ti atoms, improving the hardness and oxidation resistance of the AlTiN coating.

The average surface roughness of the substrate was 0.00744 nm as determined by AFM (Fig. 2(a)), whereas the average surface roughness of the AlTiN coating was 98.9 nm (Fig. 2(b)). The particle number for the AlTiN coating was 791; the corresponding particle area was $2.456 \times 10^5 \text{ nm}^2$, and the average diameter of the grain was 559.2 nm (Fig. 2(c)).

3.2. XPS analysis

To detect the signals for Al2P, Ti2p, N1s, O1s and C1s, a XPS full spectrum of the AlTiN coating was analyzed over the surface depth of 1 to 3 nm (Fig. 3(a)). In addition to the characteristic peaks of Al, Ti and N elements in the XPS full spectrum of the AlTiN coating, strong peaks for the O1s and C1s were noted because the coating was exposed to air. The Al content corresponded with two types of chemical environments. The binding energy of 74.12 eV corresponded with the AlN phase (a standard binding energy of 73.8 eV), and the binding energy of 74.36 eV corresponded with Al_2O_3 (a standard binding energy of 74.3 eV), as shown in Fig. 3(b). Fig. 3(c) shows that the characteristic peak of Ti was small and the peak intensity was weak. TiN and TiO_2 were detected because of the chemical environment; the binding energies of TiN and TiO_2 had been reported to be 458.90 eV and 464.85 eV for TiN and TiO_2 , respectively. Compared with the binding energy on the XPS chart, the standard binding energy of the Ti element in these two forms was 454.30 eV and 460.35 eV, respectively. The results revealed that the peak value of Ti shifted to the left by 4.60 eV when compared to the literature values for the binding energies of $\text{Ti}2p_{1/2}$ (462.1 eV) and $\text{Ti}2p_{3/2}$ (456.80 eV) in the AlTiN coating [13,14]. Therefore, the Ti2p spectrum corresponded with Ti–N in the AlTiN phase. Two situations, the AlN phase and the N–O key, were possible for the N element peak (Fig. 3(d)). The standard binding energy for AlN was 397.3 eV and that of the N–O key was 399 eV. Therefore, the N element should be in the AlN phase because the noted binding energy was 396.74 eV.

3.3. COFs and the contour of the worn trace

Under a 5 N load, the relationship between the COFs of the AlTiN coating and the wear time in the range of 700 °C–900 °C is

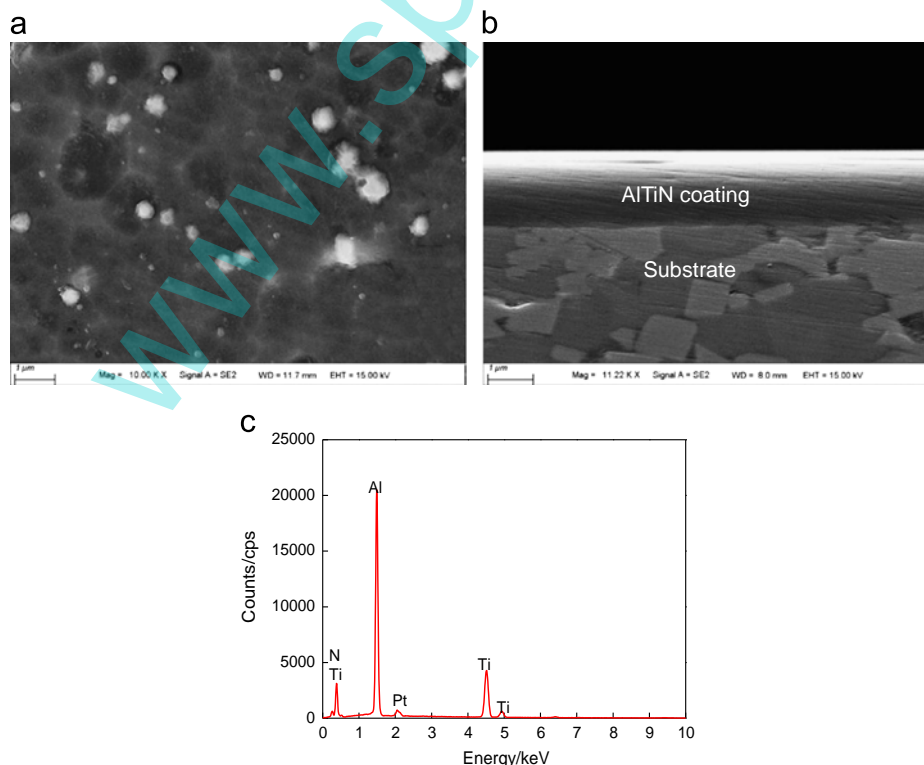


Fig. 1. Surface–interface morphologies and EDS analysis of the AlTiN coating. (a) Surface morphology; (b) Interface morphology and (c) EDS analysis. (For interpretation of the references to color in this figure legend, the reader is referred to the web version of this article.)

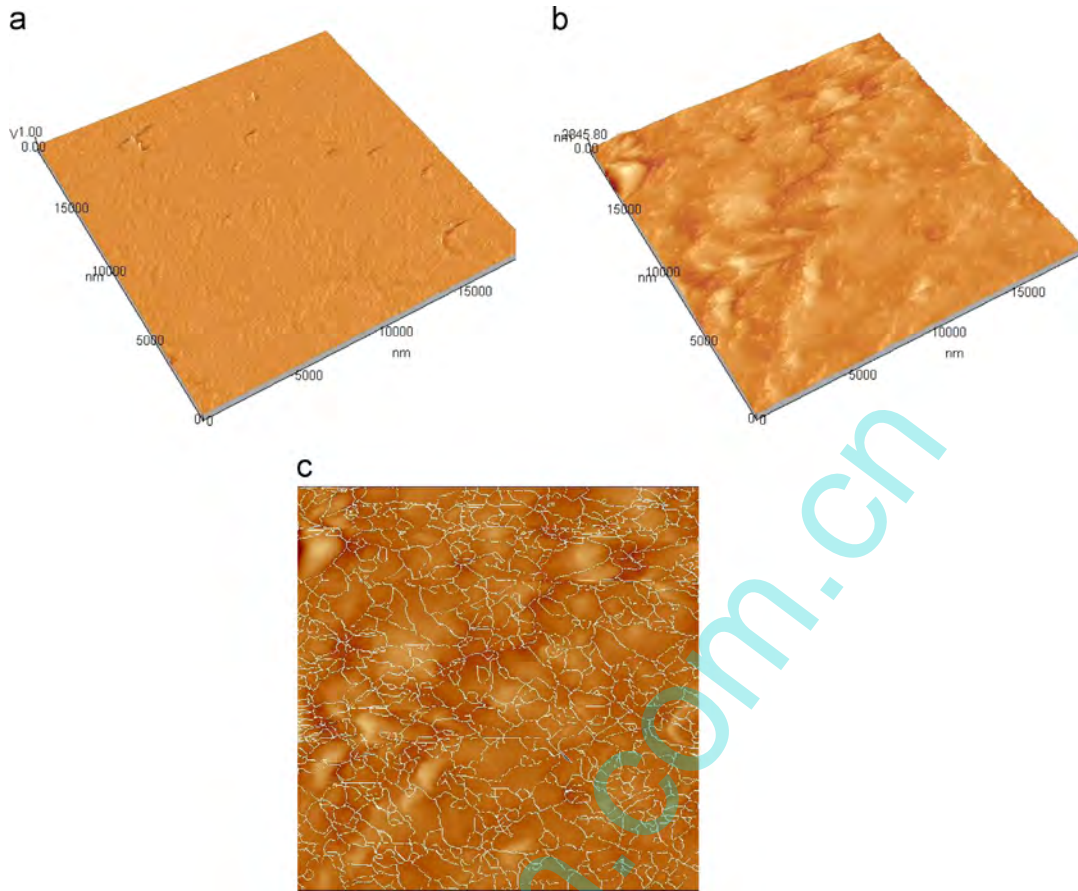


Fig. 2. AFM of the substrate and AlTiN coating surface. (a) Substrate; (b) AlTiN coating and (c) Grain size.

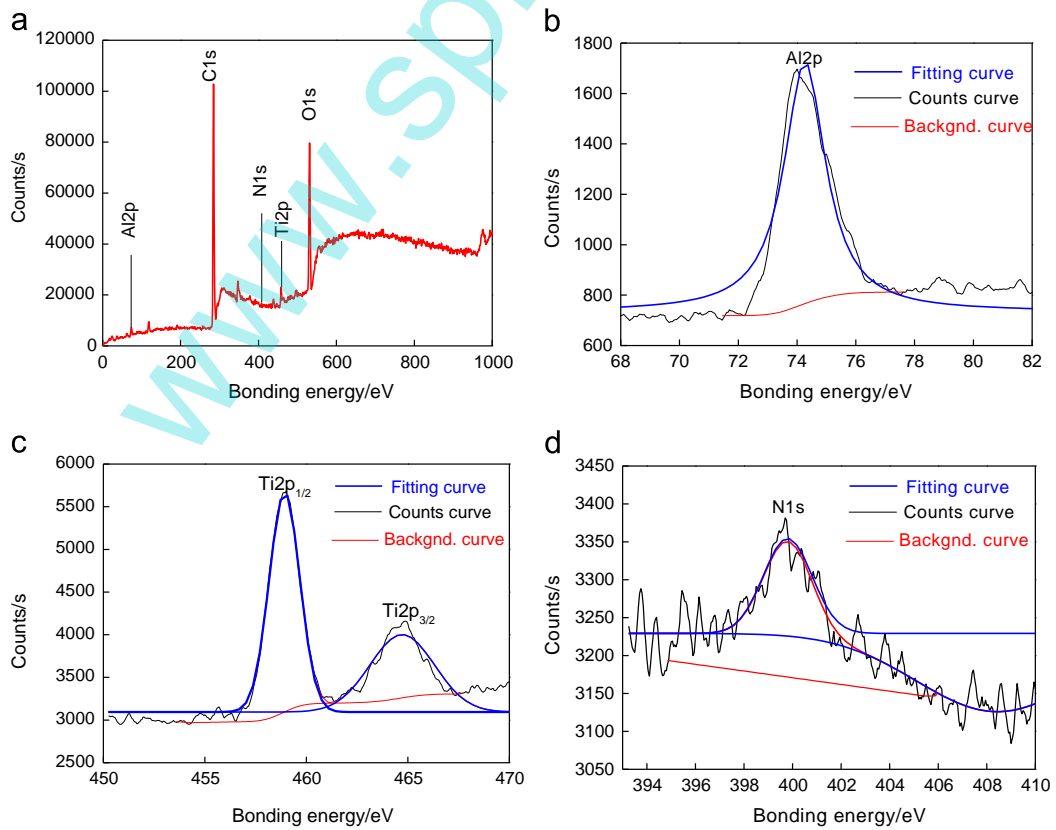


Fig. 3. XPS spectra of the AlTiN coating surface. (a) Full spectrum; (b) Al content; (c) Ti content and (d) N content.

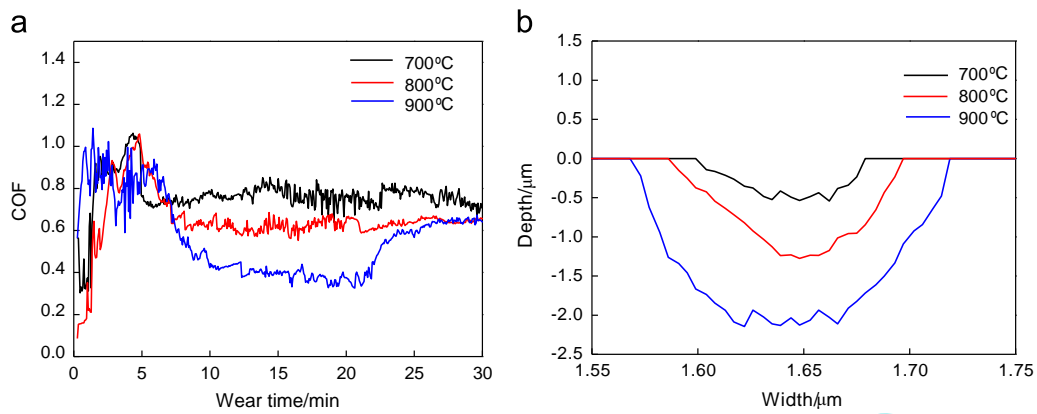


Fig. 4. COFs versus wear time and contours of the worn trace. (a) COFs versus wear time and (b) Contours of the worn trace.

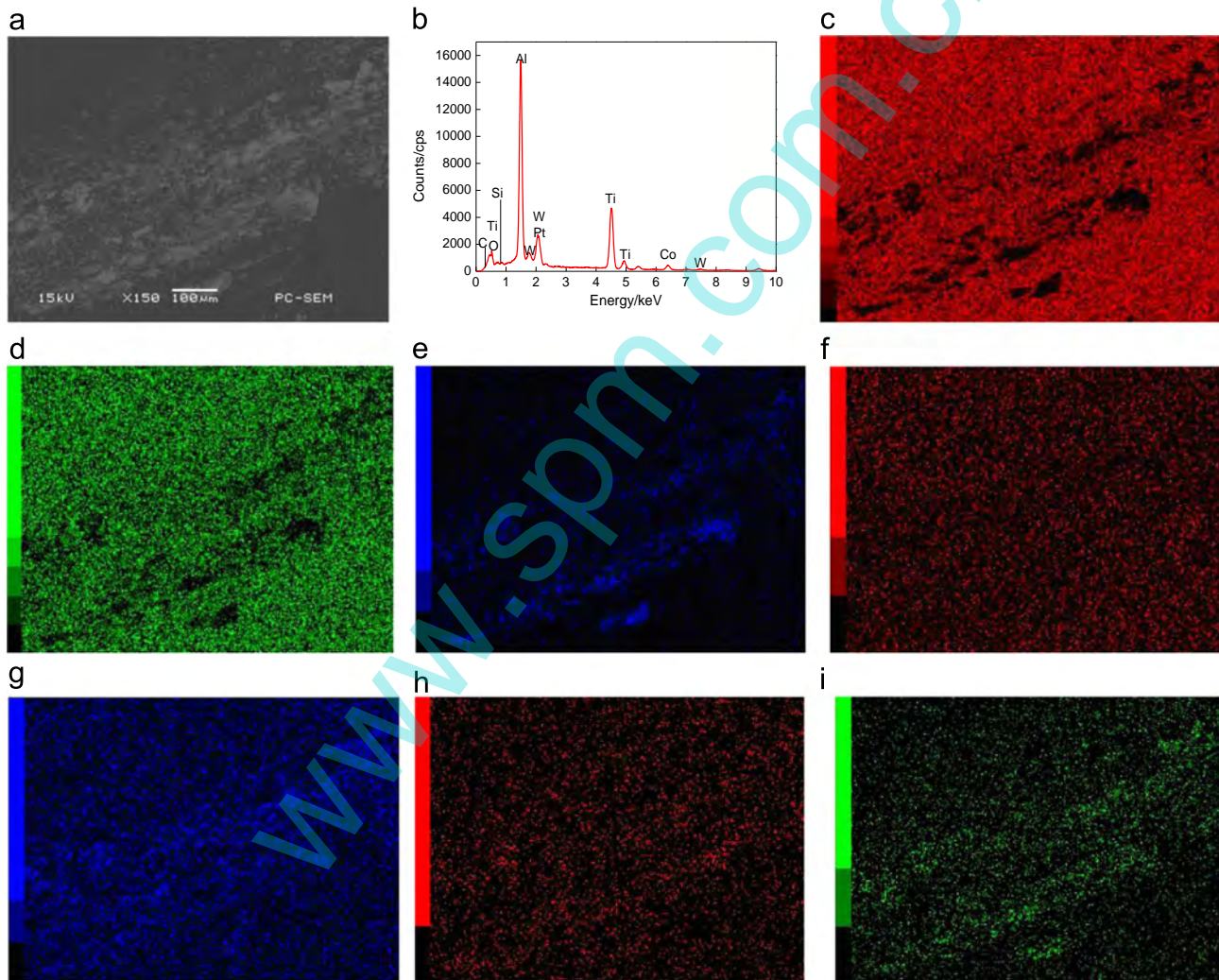


Fig. 5. Plane scans of the AlTiN coating surface at 700 °C. (a) Scanned position; (b) Result of plane scans; (c) Al content; (d) Ti content; (e) O content; (f) Si content; (g) W content; (h) C content and (i) Co content.

shown in Fig. 4(a). The average COF of the AlTiN coating was 0.77 after wearing at 700 °C for 30 min. In addition, the average COF in the running-in stage was 0.81 and was sharply increasing because the AlTiN coating surface was rough, the contact area was small, and the contacted stress was large, causing the frictional resistance to increase sharply. After the removal of surface particles, the actual contacted area increased, and the coating was oxidized to

form an oxide film layer gradually, acting as an anti-friction and lubrication effect in the wear process. Additionally, the COF began to decline slowly and tended to be gentle; the COF of the stable stage was 0.76, reducing by 6.18% when compared to the running-in stage. Because of the large fluctuations in the COF during the running-in stage and stable stage, the stability of the AlTiN coating at 700 °C was poor. At 800 °C, the average COF of the coating was

0.65, reduced by 15.38% when compared with that at 700 °C. The average COF at the running-in stage was 0.71, reduced by 11.74%, whereas the COF at the stable stage was 0.63, reduced by 17.13%. The fluctuation of COFs at the stable stage was primarily caused by the additional load and generated by the gathering of debris on the worn zone. With increasing time, the TiO₂ oxide increased, decreasing the frictional resistance; the COFs tended to be consistent; and the fluctuation decreased, showing abrasive and adhesive wear. At 900 °C, the average COF of the coating was 0.57, and the COF of the running-in stage was 0.79, reduced by 1.8% when compared with that at 700 °C. The AlTiN coating was completely oxidized to produce a large amount of Al₂O₃ and TiO₂ oxides at 900 °C, which gathered on the worn zone and formed a lubricating film. When the wear temperature increased, the COFs of the AlTiN coating decreased because the generation of TiO₂ slowed the friction and because the average COF of the stable stage was 0.40. The AlTiN coating was worn after exposing the substrate for approximately 23 min, and the COFs rose rapidly (the average COF was 0.60), showing that the AlTiN coating displayed good friction and wear properties below 800 °C and unsuitable properties at 900 °C. The contour curves of the worn traces at high temperatures are shown in Fig. 4(b). The maximum worn trace depth at 700 °C, 800 °C and 900 °C was 0.54 μm, 1.28 μm and 2.14 μm, respectively, which showed that the AlTiN coating was more worn when the temperature increased. Compared to the

AlTiN coating with a thickness of 1.75 μm, this coating was not worn at 700 °C and 800 °C. However, the depth of the worn trace was 2.14 μm at 900 °C, exceeding the coating thickness. The coating was completely oxidized and worn out to failure. Rough furrows were noted at the bottom of the worn trace under the high temperature because of the softening and oxidation of the AlTiN coating. Therefore, the grinding ball cut the oxidized coating and formed the furrow surface, increasing the wear rate of the coating. The morphologies and characteristics of the worn trace contour at the different temperatures were consistent with the fluctuations of the COF, showing that the COFs of the AlTiN coating decreased with increasing temperature, aggravating the coating oxidation wear and increasing the wear rate.

3.4. Plane scans of the worn traces

3.4.1. Plane scans of the worn trace at 700 °C

Fig. 5(a) shows the plane scans of the worn trace at 700 °C. The coating surface wore slightly, classified as slight abrasive wear. The EDS analysis result for the worn trace is shown in Fig. 5(b). The resulting mass fractions (mass, %) are as follows: Al 35.22, Ti 50.50, Si 0.77, O 8.38, W 4.67, C 0.19, and Co 0.26. Additionally, the resulting atom fractions (at, %) are as follows: Al 44.17, Ti 35.62, Si 0.93, O 17.73, W 0.86, C 0.54, and Co 0.15. Primarily Al and Ti were noted on the worn trace, and N was not detected because the N content in the

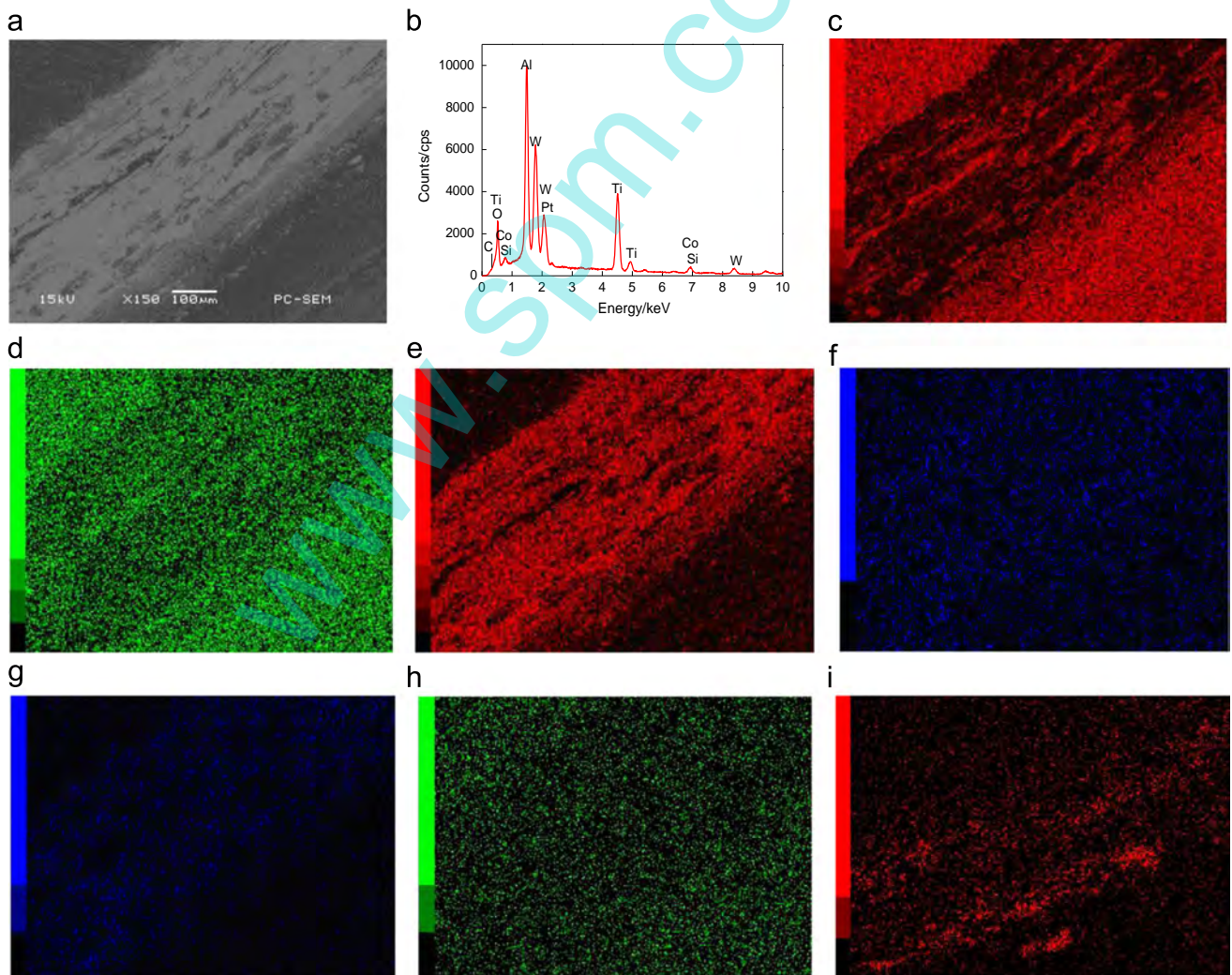


Fig. 6. Plane scans of the AlTiN coating surface at 800 °C. (a) Scanned position; (b) Result of plane scans; (c) Al content; (d) Ti content; (e) O content; (f) Si content; (g) W content; (h) C content; (i) Co content.

coating was fully released at high temperatures. Combined with Fig. 5 (c and d), the surface energy spectrum colors of the Al and Ti darkened at the worn trace, showing the occurrence of coating wear. Moreover, the O element (atom fraction of 17.73%) was detected on the worn surface, and bright zones appeared on the plane scan for the O element in Fig. 5(e), showing the partial oxidation of the AlTiN coating. A small portion of Si was also detected on the worn trace, showing that the grinding ball adhered to the coating surface and gathered on the worn zone in the form of wear debris (Fig. 5(f)). A few W, C and Co atoms resulted from the chemical elements of the substrate (Fig. 5(g–i)).

3.4.2. Plane scans of the worn trace at 800 °C

Fig. 6(a) shows the plane scans of the AlTiN coating surface at 800 °C. Compared to 700 °C, the AlTiN coating surface was more worn, and the sticking phenomenon occurred at 800 °C. The EDS analysis result for the worn trace is shown in Fig. 6(b). The resulting mass fractions (mass, %) are as follows: Al 28.61, Ti 40.63, Si 0.93, O 12.52, W 16.09, C 0.70, and Co 0.53. Additionally, the atom fractions (at, %) are as follows: Al 36.84, Ti 29.43, Si 1.15, O 27.21, W 3.04, C 2.02, and Co 0.31. The Al and Ti in the worn trace declined compared with that at 700 °C (Fig. 6(c and d)), further explaining the reduction in the atom fraction of the worn trace. The O content increased from 17.73% to 27.21% (Fig. 6(e)). The O content in the worn trace became brighter, showing that oxidation

wear and abrasive wear of the AlTiN coating occurred at 800 °C. The generated oxide film produced brittle spalling, and the debris was unable to be discharged, accumulating on the worn zone. This accumulation showed that the AlTiN removed chips poorly. The transfer occurred between the friction materials during the high temperature wear, and the grinding ball material was transferred to the worn trace because the hardness of the AlTiN coating at 800 °C was approximately 26 GPa, whereas that of the ceramic grinding ball (Si_3N_4) was only 16 GPa [15]. Furthermore, the atom fraction of Si on the worn trace increased to 1.15% at 800 °C from 0.93% at 700 °C, illustrating that Si in the worn trace was brighter (Fig. 6(f)). The contents of W, C and Co also increased significantly compared with that at 700 °C, showing that the AlTiN coating surface was more worn (Fig. 6(g–i)).

3.4.3. Plane scans of worn trace at 900 °C

Fig. 7(a) shows the plane scans of the AlTiN coating surface at 900 °C. A furrow was noted at the center of the coating surface. The EDS analysis result of the worn trace is shown in Fig. 7(b). The resulting mass fractions (mass, %) are as follows: Al 16.07, Ti 31.50, Si 1.27, O 14.73, W 34.17, C 1.63, and Co 0.64. Additionally, the atom fractions (at, %) are as follows: Al 23.68, Ti 26.11, Si 1.8, O 36.62, W 7.39, Co 5.40, and C 0.43. At 900 °C, the Al and Ti contents of the worn trace were significantly reduced compared with those at 700 °C

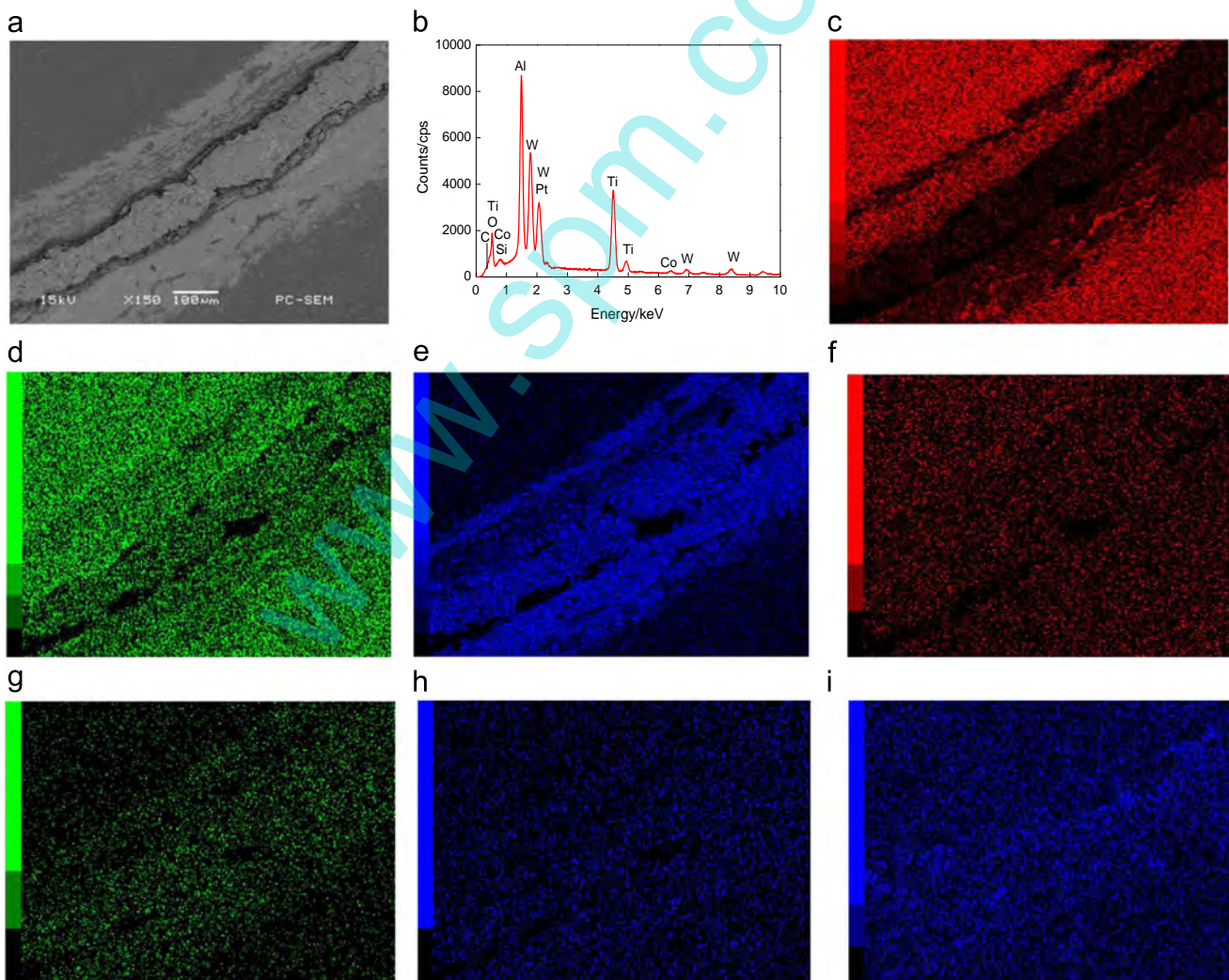


Fig. 7. Plane scans of the AlTiN coating surface at 900 °C. (a) Scanned position; (b) Result of plane scans; (c) Al content; (d) Ti content; (e) O content; (f) Si content; (g) W content; (h) C content and (i) Co content.

and 800 °C (Fig. 7(c and d)). A transfer occurred between the friction pairs at 900 °C, and the spalling debris that adhered on the worn surface was oxidized, increasing the O content (Fig. 7(e)). Moreover, the Si content of the worn trace increased and the plane scans became brighter (Fig. 7(f)). At 900 °C, the coating was more worn, and the depth of worn trace reached the substrate, producing center furrows and exposing the substrate to the air. In addition, the increase in the contents of W, C and Co further indicated that the coating was

completely oxidized at 900 °C, and the AlTiN coating failed to function at this temperature (Fig. 7(g–i)).

3.5. Wear mechanism

3.5.1. Worn morphologies

Fig. 8 shows the worn morphologies of the AlTiN coating at 700 °C. The worn traces were divided into debris adhesion and debris

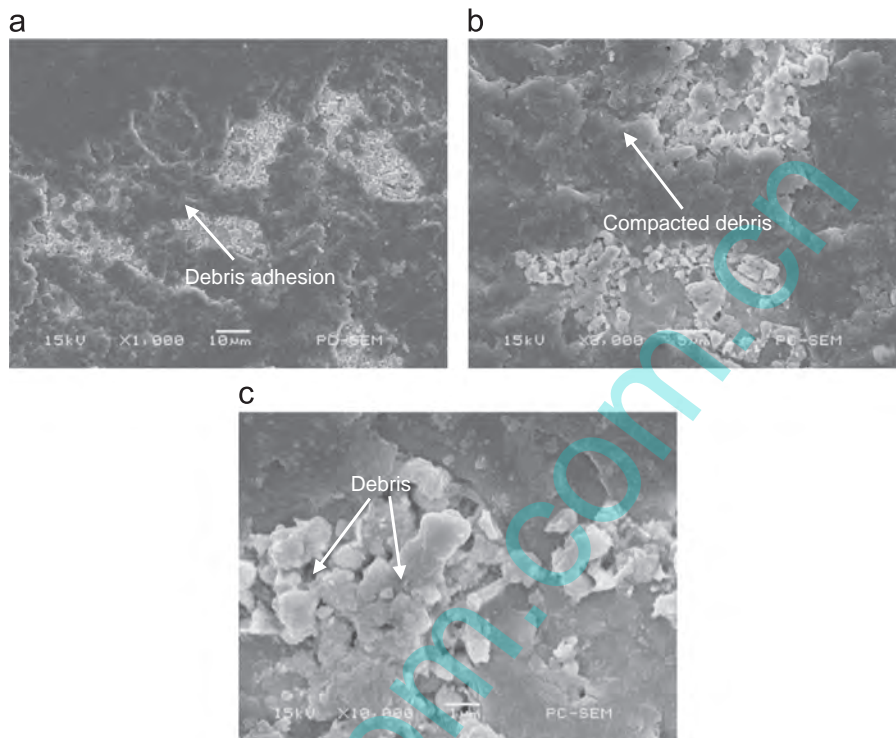


Fig. 8. Worn morphologies of the AlTiN coating at 700 °C. (a) Low magnification; (b) Medium magnification and (c) High magnification.

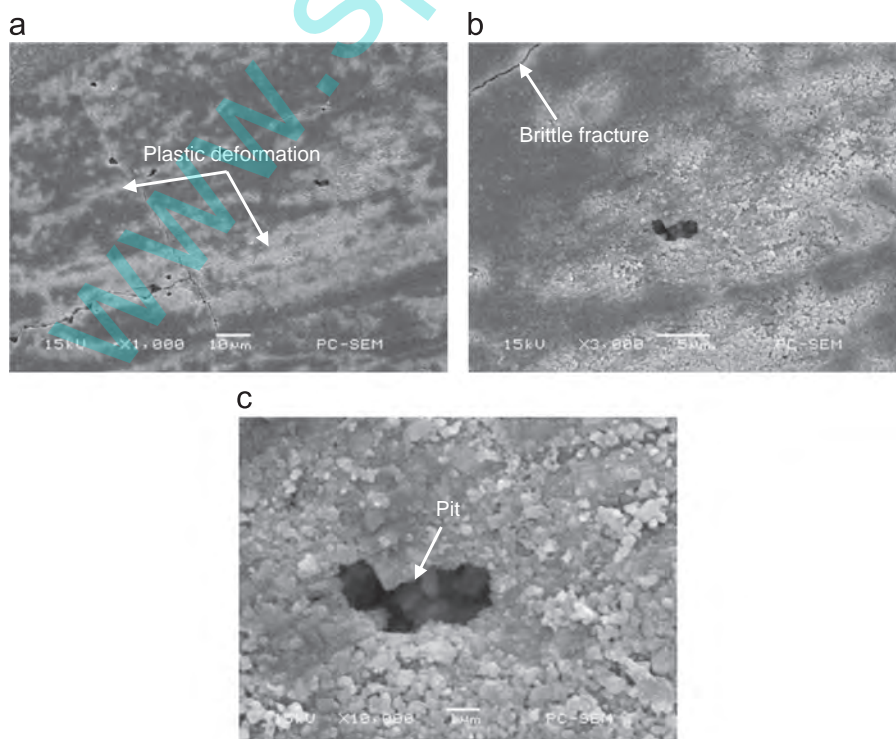


Fig. 9. Worn morphologies of the AlTiN coating at 800 °C. (a) Low magnification; (b) Medium magnification and (c) High magnification.

compaction. As shown in Fig. 8(a), the debris adhered with an intensive scale shape on the worn surface at the high temperature, The AlTiN coating produced a substantial amount of debris during the wear, showing the adhesion wear mechanism. The debris was unable to be discharged and was continuously compacted under the

cycle load, forming a rough surface (Fig. 8(b)). The worn particles (white light) were smaller because the Al content in the AlTiN coating exceeded the Ti content. Therefore, the oxidation products were primarily Al_2O_3 , with a lower amount of TiO_2 . Furthermore, the generated mixed-oxide film had a good bearing capability,

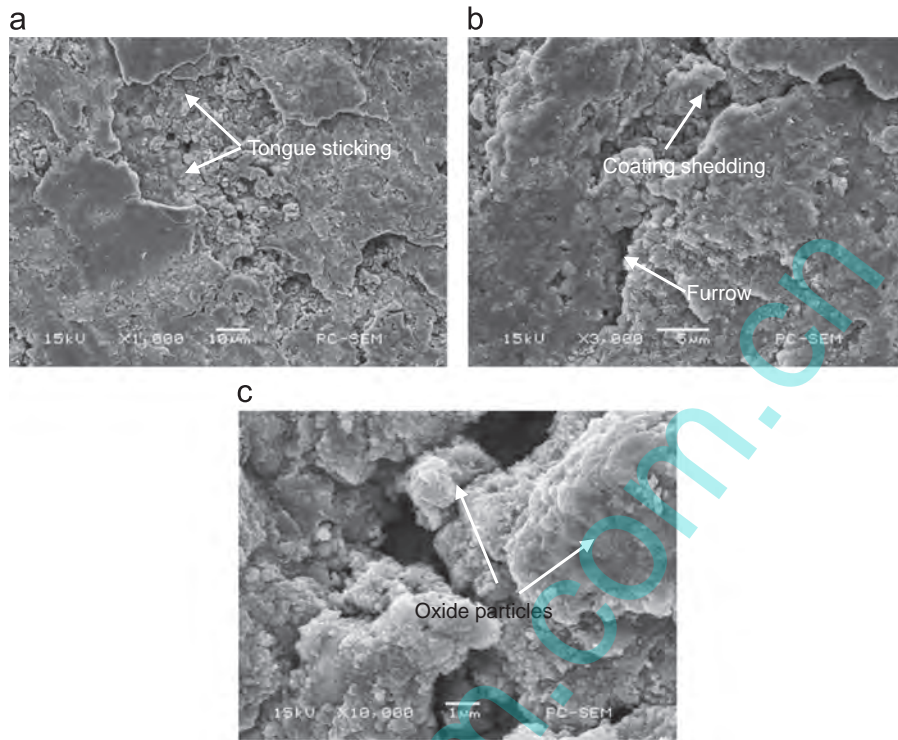


Fig. 10. Worn morphologies of the AlTiN coating at 900 °C. (a) Low magnification; (b) Medium magnification and (c) High magnification.

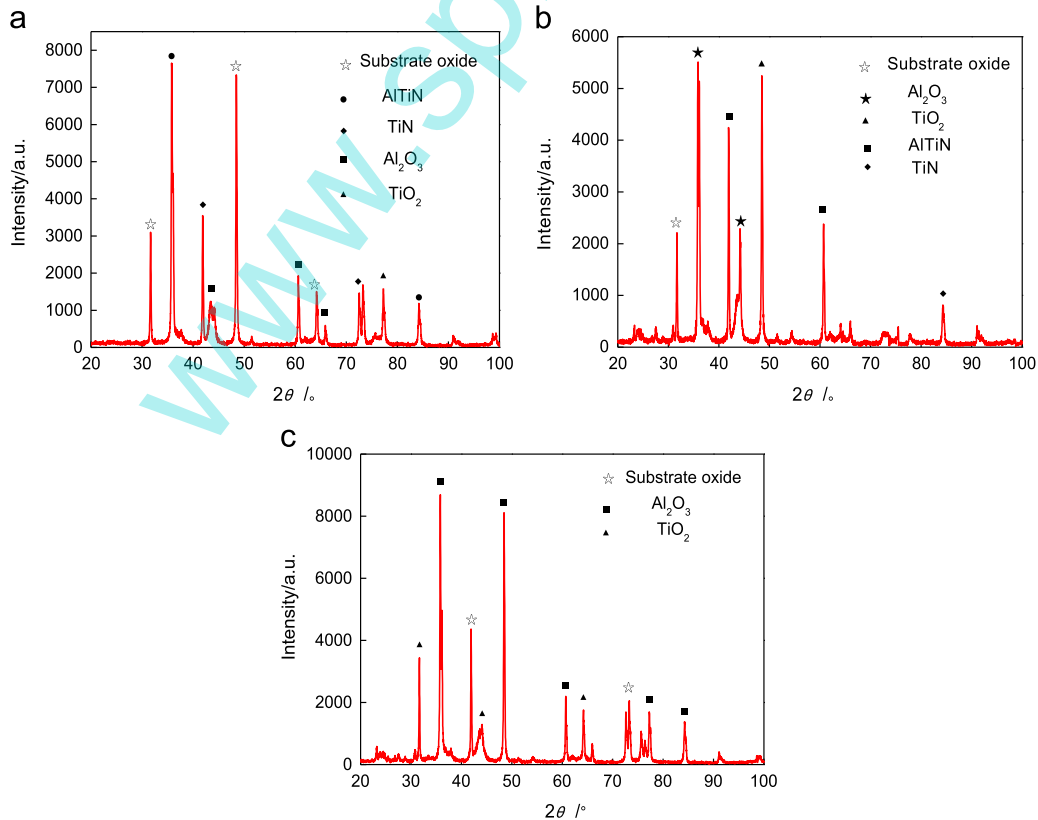


Fig. 11. XRD analysis of the AlTiN coatings at different temperatures. (a) 700 °C; (b) 800 °C and (c) 900 °C.

compactness and antioxidant ability. These factors played an important role in protecting the AlTiN coating (Fig. 8(c)).

Fig. 9 shows the worn morphologies of the AlTiN coating at 800 °C. During the wear, the O atoms in the air were diffused to the AlTiN coating and the Al atom was diffused towards the coating surface. The Al atoms combined with the O atoms to form a compact and high thermally stable Al_2O_3 at the high temperature. Moreover, the lamination phenomenon on the surface layer was high for Al and low for Ti, whereas the oxides in the inner layer were abundant for Ti and scarce for Al [16]. Because of the low shearing strength of TiO_2 and the high strength of Al_2O_3 , the TiO_2 displayed a lubricating effect whereas the Al_2O_3 displayed wear resistance and high temperature oxidation resistance on the AlTiN coating. As shown in Fig. 9(a), few obvious folds were noted because the debris adhesion or the coating became soft and deformed at the high temperature. Brittle fractures of the coating were found on the worn trace in Fig. 9(b), displaying that under the circular contact, the AlTiN coating cracked because of stress fatigue and the crack expanded gradually. Therefore, the coating produced a fracture phenomenon, showing a fatigue wear mechanism. Moreover, pits were found on the AlTiN coating surface because large droplets were dragged by the ceramic ball, leaving the coating surface (Fig. 9(c)).

Fig. 10 shows the worn morphologies of the AlTiN coating at 900 °C; the AlTiN coating was seriously worn. The ligule adhesion was noted on the worn trace because the Al had a strong chemical activity at the high temperature. Additionally, the high Al content in the AlTiN coating was ensured to improve the adhesion between the friction pairs (Fig. 10(a)). The flaking and deep furrows were also noted on the worn trace in Fig. 10(b) because the oxide film generated a substantial amount of hard flaking debris during the brittle breaking under the load. This hard abrasive dust was pressed into the friction surface. In addition, the debris cut the coating surface when sliding. Therefore, furrows were formed on the coating surface, accelerating the wear of the coating and showing an abrasive wear mechanism. In addition, the oxidative denaturation of the coating also caused the coating to shed (Fig. 10(c)). The volume of the AlTiN coating expanded after oxidation. Because the thermal expansion of the coating and substrate were mismatched, the coating easily fell off. Therefore, the wear mechanism of the AlTiN coating was primarily composed of oxidation wear and abrasive wear, accompanied with adhesive wear and fatigue wear.

3.5.2. XRD analysis

Fig. 11 shows the XRD patterns of the AlTiN coatings at 700 °C, 800 °C and 900 °C. The substrate was oxidized, and the oxides emerged on the substrate. The diffraction peaks for AlTiN and TiN were detected on the coating at 700 °C and 800 °C; both compounds displayed FCC (face-centered cubic) structure of B1-NaCl [17]. The emergences of Al_2O_3 and TiO_2 diffraction peaks displayed that the AlTiN coating had been partially oxidized during the wear. Moreover, the diffraction peaks of Al_2O_3 had a higher intensity compared with that of TiO_2 because the Al atom had a strong affinity to the O atoms and the Gibbs free energy required for forming Al_2O_3 was low. Therefore, Al_2O_3 was preferentially generated when compared to TiO_2 . The Al_2O_3 could provide a protective effect for the coating and further slow the oxidation, increasing the wear resistance of the AlTiN coating (Fig. 11(a and b)). The diffraction peaks of AlTiN and TiN were absent until 900 °C. Additionally, numerous strong diffraction peaks were noted for Al_2O_3 and TiO_2 , showing that the coating had been completely oxidized (Fig. 11(c)).

4. Conclusions

(1) The N content of the AlTiN coating is fully released at high temperatures to form the two mixed oxide films of Al_2O_3 and TiO_2 , in which the TiO_2 plays a lubricating effect and the Al_2O_3

provides wear resistance and oxidation resistance at high temperatures.

- (2) At 700 °C, 800 °C and 900 °C, the average COF of the AlTiN coating is 0.77, 0.65 and 0.57, respectively, and the COFs of the AlTiN coatings decrease with increasing temperatures, aggravating the oxidation wear and causing the wear rate increase.
- (3) The wear mechanisms of the AlTiN coating at high temperatures are primarily composed of oxidation wear and abrasive wear, accompanied by fatigue wear and adhesive wear. Additionally, the coating is oxidized and failed with increasing temperatures; the coating fails to function at 900 °C.

Acknowledgments

Financial support for this research by the Jiangsu Province Science and Technology Support Program (Industry) (BE2014818) is gratefully acknowledged.

Appendix A. Supporting information

Supplementary data associated with this article can be found in the online version at <http://dx.doi.org/10.1016/j.triboint.2015.03.009>.

References

- [1] Liang, Li Yang, Xian Chen, Ying Zhang, Yuqing Zhao. Effects of chromium, titanium and aluminum on the friction and wear properties of nitride hard coatings. *Vacuum* 2012;49(2):47–51.
- [2] Changjun Zhu, Kanghua Chen, Shequan Wang, Yinchao Xu, Canqiang Xie, Xiangming Chen. Effects of gradient substrate structure on oxidation resistance of TiN coated cemented carbide. *J Cent South Univ (Sci Technol)* 2011;42(10):2984–9.
- [3] Bin Tian, Wen Yue, Zhiqiang Fu, Yanhong Gu, Chengbiao Wang, Jiajun Liu. Microstructure and tribological properties of W-implanted PVD TiN coatings on 316 L stainless steel. *Vacuum* 2014;99:68–75.
- [4] Dejun Kong, Yongzhong Fu, Yongzhong Wu, Wenchang Wang. Surface and interface properties of TiN films grown by physical vapor deposition. *Chin J Vac Sci Technol* 2012;32(12):1078–83.
- [5] Gang Tan, Guangbin Zhao, Fanguan Liao, Lei Luo, Xiaojian Ai, Di He. Preparation and properties of TiAlN film by MF magnetron sputtering. *Vacuum* 2014;51(2):56–9.
- [6] Ramadoss Radhika, Kumar N, Pandian R, Dash S, Ravindran TR, Arivuoli D, et al. Tribological properties and deformation mechanism of TiAlN coating sliding with various counterbodies. *Tribol Int* 2013;66:143–9.
- [7] Juncai Liang, Wuping Zhou, Jiangang Zhang, Fengge Mu, Haibo Zhao. Evolution analysis of existing forms of Ti and Al elements during preparation of TiAlN coating. *Chin J Rare Met* 2014;38(4):561–6.
- [8] Wang Mei, Toihara Takaomi, Sakurai Masatoshi, Kurosaka Wataru, Miyake Shojiro. Surface morphology and tribological properties of DC sputtered nanoscale multilayered TiAlN/CNx coatings. *Tribol Int* 2014;73:36–46.
- [9] Zhiwen Xie, Langping Wang, Jiuchun Wang, Xiaofeng Yan, Lei Huang, Yang Lu. High temperature oxidation resistance and wear properties of TiAlN coatings deposited by MPEHD 2011;31(2):175–80. *Tribology* 2011;31(2):175–80.
- [10] Dejun Kong, Guizhong Fu. Friction and wear behaviors of AlTiCrN coatings by cathodic arc ion plating at high temperatures. *J Mater Res* 2015;30(4):503–11.
- [11] Ramadoss Radhika, Kumar N, Pandian R, Dash S, Ravindran TR, Arivuoli D, et al. Tribological properties and deformation mechanism of TiAlN coating sliding with various counter bodies. *Tribol Int* 2013;66:143–9.
- [12] Beake BD, Fox-Rabinovich GS. Progress in high temperature nanomechanical testing of coatings for optimising their performance in high speed machining. *Surf Coat Technol* 2014;255:102–11.
- [13] Strydom Le R, Hofmarm S. The contribution of characteristic energy losses in the core-level X-ray photoelectron spectroscopy peaks of TiN and (Ti, Al)N studied by electron energy loss spectroscopy and X-ray photoelectron spectroscopy. *J Electron Spectrosc Relat Phenom* 1991;56:85–103.
- [14] Barshilia Harish C, Yogesh K, Rajam KS. Deposition of TiAlN coatings using reactive bipolar-pulsed direct current unbalanced magnetron sputtering. *Vacuum* 2009;83:427–34.
- [15] Yang Q, McKellar R. Nanolayered CrAlTiN and multilayered CrAlTiN–AlTiN coatings for solid particle erosion protection. *Tribol Int* 2015;83:12–20.
- [16] Biksa A, Yamamoto K, Dosbaeva G, Veldhuis SC, Fox-Rabinovich GS, Elfizy A, et al. Wear behavior of adaptive nano-multilayered AlTiN/Me_xN PVD coatings during machining of aerospace alloys. *Tribol Int* 2010;43(8):1491–9.
- [17] Birol Yucel. Sliding wear of CrN, AlCrN and AlTiN coated AISI H13 hot work tool steels in aluminium extrusion. *Tribol Int* 2013;57:101–6.